Multiple Linear Regression Analysis for Prediction of Pressure Drop in Gas-Solid Fluidized Bed

Saikat Banerjee
College of Engineering and Technology, Engineering Department, University of Technology and Applied Sciences

Selvaraju Sivamani
College of Engineering and Technology, Engineering Department, University of Technology and Applied Sciences

Naveen Prasad B S
College of Engineering and Technology, Engineering Department, University of Technology and Applied Sciences

Vasu Gajendiran
College of Engineering and Technology, Engineering Department, University of Technology and Applied Sciences

https://doi.org/10.5109/7342441

出版情報：Evergreen. 12 (1), pp.90-103, 2025-03. Interdisciplinary Graduate School of Engineering Sciences, Kyushu University, Japan
バージョン：

Multiple Linear Regression Analysis for Prediction of Pressure Drop in Gas-Solid Fluidized Bed

Saikat Banerjee[1], Selvaraju Sivamani[1], Naveen Prasad B S[1,*], Vasu Gajendiran[1]
[1]College of Engineering and Technology, Engineering Department,
University of Technology and Applied Sciences, Salalah, Oman

*Author to whom correspondence should be addressed:
E-mail: bsnaveenprasad@gmail.com

(Received October 5, 2024; Revised January 10, 2025; Accepted January 16, 2025).

Abstract: Fluidized beds have widespread applications in industrial processes, including gas-solid operations like coal combustion, catalytic reactions such as petroleum cracking, and as bioreactors. The goal of this study is to look into how flow behaves in a fluidized bed using an air-solid system and ballotini using multiple linear regression analysis. Employing a multiple linear regression analysis for fluidized bed systems helps figure out how the independent and dependent variables are related. This lets you know how much each independent variable affects the dependent variable while keeping the other variables' effects in check. This helps in understanding complex interactions, predicting outcomes, and identifying key factors that significantly affect the dependent variables. Different bed heights (0.5 to 1.5 m) and gas speeds (0.02 to 0.12 m/s) were used to find response variables such as pressure drop per unit bed height, friction factor, power consumption, and drag coefficient. From the results, it could be concluded that when the model is applied, the differences between the residuals also tend to follow a normal distribution for most of the data points.

Keywords: Fluidization; Air-ballotini system; Superficial gas velocity; Bed height; Pressure drop; Friction factor; Power consumption

1. Introduction

Fluidized beds are widely utilized in industrial processes, including gas-solid reactions such as coal combustion and catalytic reactions like petroleum cracking. These systems are essential for enhancing contact between gases and solids, characterized by high velocities and significant fluid-solid surface areas per unit volume[1)]. Fluidized particles frequently collide with one another and with the walls of the container, leading to substantial phase interactions. Although the significance of liquid-particle and particle-particle interactions in liquid-solid fluidization is acknowledged, research in this domain is still scarce, especially concerning flow stability and resistance in liquid-solid systems. While the importance of liquid-particle and particle-particle interactions in liquid-solid fluidization is recognized, research in this area remains limited, particularly regarding flow stability and resistance in liquid-solid systems. The dynamics of wet particles are critical, as the liquid bridges between particles greatly influence the overall system behavior, underscoring the need for a deeper understanding to optimize reactor design and processes[2)].

Recent interest in fluidized beds has surged, driven by new applications for fine particles and the rising significance of circulating fluidized beds and high-velocity systems. Numerous studies continue to explore advancements in fluidization technology. This review focuses primarily on gas-solid systems, as liquid-solid fluidized beds are less prevalent in research and practice[3,4)]. Moreover, topics such as solids flow in standpipes and pneumatic conveying are excluded, as they are typically associated with auxiliary fluidized bed equipment. The emphasis is placed on hydrodynamics and solids mixing within gas-solid fluidized beds, while heat and mass transfer, as well as reactor modeling, are beyond the scope of this discussion[5,6)].

A stable and well-designed experimental apparatus is crucial for investigating fluid flow in particle beds. Such a system typically consists of two transparent, removable columns that allow simultaneous monitoring of water and air flow. Pressure gauges display the pressure drop across the bed, with water pumped through a flow meter and air supplied by a compressor. Different-sized glass beads can be utilized as bed materials[7,8)]. Fluidized beds, which consist of two-phase mixtures of fluid and particulate solids, are integral to various technological processes, including hydrocarbon cracking, coal gasification, ore roasting, Fischer-Tropsch synthesis, and polyethylene production. They also serve functions in waste combustion, nuclear fuel preparation, and the drying, cooling, heating, and transport of solid materials[9,10].

The concept of a fluidized bed is intimately connected to particulate solids, which are formed through both natural processes, like erosion and thermal expansion, and technological methods such as grinding and crystallization. Inorganic particulate materials often exhibit a wide range of particle sizes, termed polydisperse materials, while organic particles, such as seeds and fruits, are typically more uniform and classified as monodisperse materials. Notable studies, such as those by Kaewklum et al. (2009), have investigated hydrodynamic regimes in vortex fluidized bed combustion using various particle sizes of quartz sand. Their experiments, utilizing a spiral vortex air diffuser, explored air-sand flow properties across different operating conditions, highlighting the complex interactions within fluidized beds. Fluidized beds are vital in modern chemical engineering, facilitating numerous physical and chemical processes. Continued research is essential to enhance understanding and optimization of these systems, particularly in gas-solid applications, to leverage their full potential in industrial settings[11,12].

Ju et al. (2019) developed a dynamic model for a dual fluidized-bed CO_2 capture system, focusing on regeneration energy and capture efficiency. They used a potassium carbonate sorbent and found that capture efficiency dropped to 18.6% with CO_2 regeneration due to incomplete sorbent regeneration, while using nitrogen at 150°C reduced efficiency only slightly, from 52.8% to 51.9%. Optimizing regeneration conditions improved capture efficiency to 73.2% at 160°C, requiring 234.8 kJ/mol CO_2. Lowering the temperature below 145°C cut energy consumption to around 200 kJ/mol CO_2, maintaining operational capacity[12] . The model aids in enhancing energy efficiency. While fluidized bed systems have been extensively studied, there remains a lack of comprehensive understanding of the quantitative relationships among various operational parameters and their effects on flow behavior. There is a need for more multivariate analysis that looks at how parameters like bed height and superficial gas velocity affect each other and how they affect pressure drop, friction factor, power consumption, and drag coefficient. A lot of the research that has been done so far has focused on qualitative observations or single variables[13-15].

This study introduces a novel approach by applying multiple linear regression analysis to a comprehensive air-solid fluidized bed system using ballotini, allowing for a systematic evaluation of the interrelationships between key operational parameters. By quantifying these relationships, the research enhances predictive modeling capabilities and offers a refined understanding of the complex dynamics within fluidized beds, contributing new insights that can improve the design and operation of industrial processes. From the identified research gap and novelty statement, the aim of this study is to quantitatively investigate the flow behavior in an air-solid fluidized bed system using multiple linear regression analysis to elucidate the relationships among critical parameters affecting operational performance. The objectives are as follows: (i) To identify and quantify the influence of independent variables (bed height and superficial gas velocity) on dependent variables (pressure drop per unit bed height, friction factor, power consumption, and drag coefficient) in a fluidized bed system; (ii) To employ multiple linear regression analysis to develop predictive models that accurately represent the relationships among these variables; and (iii) To assess the normality of residuals from the regression analysis to validate the robustness of the model and ensure reliable predictions.

2 Materials and Methods

2.1 Materials:

Ballotini was kindly provided by Armfield Limited, Hampshire, England. Air was supplied by using compressor (Armfield Limited, England). Armfield Engineering Fixed and Fluidized Bed Apparatus (CEL-MKII) was used for fluidization studies of air-ballotini system.

2.2 Experimental set-up:

Figure 1 shows a schematic diagram of the experimental setup. The column, made of acrylic, has an internal diameter of 50 mm and a maximum height of 600 mm. It is divided into two sections: one for gas or liquid distribution and the other for liquid discharge. The setup includes two transparent beds, rotameters, manometers, a low-pressure air source, and the necessary valves and fittings. An air vent is located at the bottom of the column. The test section features wire mesh at both the top and bottom to prevent particle elutriation. Manometer taps are installed to measure the pressure drop across the column, and provisions are made to facilitate the loading and unloading of solid particles. A control valve is installed in the discharge line to regulate flow rate

.

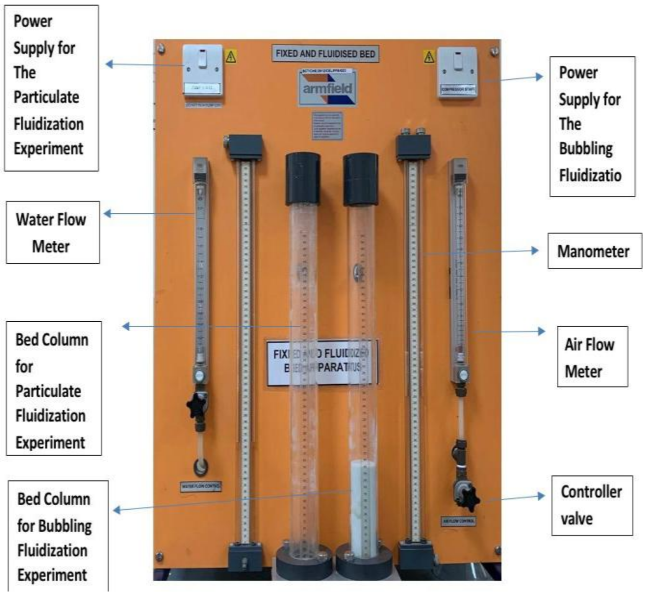

Fig. 1: Fixed and fluidised bed column.

2.3 Experimental procedure and calculation:

The solid particles (ballotini) were introduced through the loading provision in the test section for various bed heights ranging from 0.5 to 1.5 m. The compressor was then started to supply air at the required flow rate, fully fluidizing the particles. Afterward, the air flow rate was gradually reduced until the solids slowly settled to form a packed bed, representing the initial bed height. The air flow rate was then gradually increased, and the corresponding changes in bed height were observed. The flow rate at which the bed height first began to change was recorded. A manometer using water as the manometric fluid was used to measure the pressure drop across the column[16)]. For each measured flow rate and bed height, the corresponding manometer readings were recorded, and the pressure drop was calculated. Additionally, a manometer with water as the manometric fluid was also used. From these readings, various parameters were calculated, including the pressure drop, friction factor, drag coefficient (CD), superficial gas velocity, and power number. The pressure drop (ΔP) for fluid flow through a fluidised bed in a column containing air-solid particles is a key hydrodynamic parameter that is determined[17)] by the following Equation (1).

$$\Delta P = (1-\varepsilon)\,(\rho_p-\rho_a)\; g.h \qquad (1)$$

where ΔP = Pressure drop, ϵ = Void fraction of bed, ρ_p = Particle density, ρa = Particle density, and h = Height of the bed,

The solid particles become entrained when the upward fluid velocity is high enough, causing them to be carried along with the air and the superficial gas velocity (v) for fluidised bed is calculated[15,17)] by the following Equation (2),

$$v = \mathcal{Q}/\mathcal{A} \qquad (2)$$

where $\mathcal{Q}$ = Volumetric flow rate of air, and $\mathcal{A}$= Cross sectional area of the bed,

The Friction Factor (F) for a fluidized bed can be determined through specific calculations. This involves considering various parameters such as the fluid properties, particle characteristics, and flow conditions within the bed[15,17)]. By applying appropriate mathematical models or empirical correlations, the friction factor can be calculated to quantify the resistance encountered by the fluid as it moves through the bed of solid particles by using Equation (3),

$$F = 150/Nrep + 1.75 \qquad (3)$$

where $Nrep$ = Particle Reynolds number.

Power consumption typically refers to the electrical energy used to operate an appliance over a period. Energy or friction losses, on the other hand, describe the pressure difference needed to overcome resistance during fluid flow through pipes. These losses occur solely due to dynamic movement, meaning they can be considered a form of dynamic differential pressure. As a result, friction losses only happen when there is actual flow[17)]. The power consumption was calculated using Equation (4),

$$P = \Delta P \times \mathcal{Q}/\varepsilon \qquad (4)$$

where P = Power consumption, ΔP = Pressure drop, $\mathcal{Q}$ = Volumetric flow rate of air, and ϵ = Void fraction of bed.

The Drag Coefficient for a fluidized bed refers to a key dimensionless parameter that characterizes the resistance or drag force experienced by solid particles as they interact with the fluid moving through the bed. This coefficient is influenced by factors such as particle size, shape, and density, as well as the fluid's velocity, viscosity, and flow regime. The drag coefficient plays a crucial role in determining the dynamics of particle-fluid interaction, affecting the stability, fluidization behaviour, and overall efficiency of the fluidized bed system[17)] by calculating the drag coefficient ($\mathcal{CD}$), as given in Equation (5),

$$\mathcal{CD} = 0.4 + 24/Nrep \qquad (5)$$

where $Nrep$ = Particle Reynolds number.

Accurate calibration, high repeatability, and minimal error margins are vital for the reliable operation of manometers and flowmeters in gas-solid fluidized bed systems. Calibration aligns instrument readings with standard reference values, ensuring precise pressure measurements in manometers and accurate flow rate readings in flowmeters. Repeatability to produce identical readings under the same conditions, is essential for maintaining process control and research reliability. Error margins, influenced by factors like sensor precision and calibration quality, quantify deviations from true values.

All runs were made at room temperature (25±2°C). Reducing these margins enhances accuracy, supporting effective fluidization and optimizing operational performance in fluidized bed systems.

2.4. Multiple linear regression analysis:

Multiple regression analysis encompasses a range of techniques utilized to investigate linear relationships among two or more variables. The variables in the Equation (6) are estimated through this analysis. In this context, the independent variables are denoted as x, while y represents the dependent variable. The subscript j indicates the observation number for each row. The regression coefficients, which remain unidentified, are symbolized by A, and their estimates are represented by E. The parameter A approximates each unknown population parameter. The residual or error for observation j is minimized[18-20].

$$y_j = A_0 + A_1 x_{1j} + A_2 x_{2j} + \ldots\ldots\ldots + A_p x_{pj} + E_j \quad (6)$$

Additionally, the count, minimum and maximum values, standard deviation, and arithmetic mean for each variable are calculated, facilitating appropriate variable selection. This section also provides the values of regression coefficients along with significance tests, thereby evaluating the accuracy of the hypotheses. It is important to note that collinearity may distort the magnitude or sign of the regression coefficients as well as the results of the t-test. The t-test evaluates all other x variables, comparing the alternative hypothesis, $A_j = 0$, against the null hypothesis, $A_j \neq 0$. The corresponding t-value has n - p - 1 degrees of freedom[21-23].

3.RESULTS AND DISCUSSION

The following section lists the independent variables involved. The regression coefficients, estimated through the least squares method, indicate the extent to which y changes with each unit increase in x, assuming all other x variables remain constant. These coefficients are sometimes referred to as partial-regression coefficients due to the diminished influence of other x variables.

3.1 Pressure drop per unit bed height

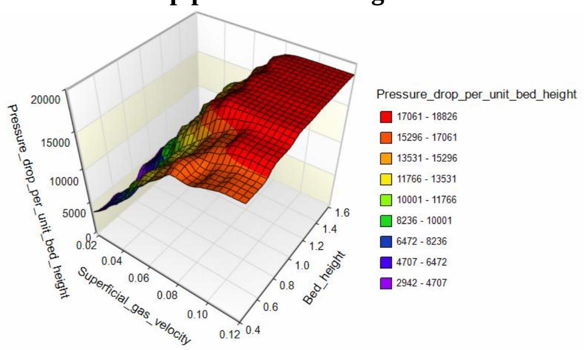

Fig. 2: Surface plot of pressure drop per unit bed height in N/m^3 superficial gas velocity in m/s and bed height in m.

Figure 2 shows surface plot of pressure drop per unit bed height in N/m^3 superficial gas velocity in m/s and bed height in m. Surface charts show numerical data in three dimensions. The functional relationship between two independent variables and a dependent variable (the volume of hydrogen produced) is displayed using surface plots[24]. It is essential to comprehend plot construction. This study generates a two-dimensional grid of bed height and surface gas velocity. Grid range and data range coincide. Next, an estimate of each grid point's volume is given[25].

The bed height pressure reduction is calculated using the weighted average of all data values near this grid point. The number of points to average is up to the user. Using these averaged values, the three-dimensional surface is constructed. The variance at each grid point is not well represented by the surface plot[26,27]. The relationship between a dependent variable and two independent variables is displayed in these graphs using regression analysis. Keep in mind that this surface is assumed to be flat for multiple regression. It is simpler to determine whether multiple regression is required when using surface plots[28].

The gas passes through the gaps between the particles at low surface gas velocities without causing any noticeable movement in them. There is not much of a pressure decrease and the bed stays in its fixed position.

When the gas velocity rises, it eventually reaches a point where the particles' downward gravitational force and the gas's upward drag force are equal. This is referred to as the minimal velocity of fluidization. At this moment, the bed starts to behave like a fluid as particles start to lift and move. The bed is entirely fluidized when it reaches the minimum fluidization velocity. The bed has qualities similar to a fluid, and the particles are suspended in the gas stream. The weight of the particles mostly controls the rather consistent pressure drop over the bed as followed by other researcher[29,30].

The bed transitions into a turbulent fluidization phase with even higher gas velocities. The bed gets increasingly disorganized as the particles travel faster. Particles are carried out of the bed by the gas stream in a fast fluidization regime that can be reached if the velocity keeps rising. Up to the point of lowest fluidization, the pressure drop across the bed increases with surface gas velocity. Even with additional increases in gas velocity, the pressure decrease stabilizes and stays mostly constant after fluidization. Designing and improving fluidized bed reactors, which are widely utilized in numerous industrial processes such chemical reactions, drying, and particle coating, requires an understanding of these effects[31,32].

Below is the approximated Equation (7) that fits the curves: P is pressure drop throughout the bed height, L is bed length, and G is super gas velocity.

$$\Delta P/L = 411.35 + 147455.5\,G + 2623.57\,L \quad (7)$$

The Equation 7 is generated from the experimental data for which the Fig. 2 is plotted. This shows the validation of the equation.

The regression coefficient T test is presented in Table 1 for pressure drop per unit bed height in N/m^3 superficial gas velocity in m/s and bed height in m and the details of the analysis of variance are presented in Table 2 pressure drop per unit bed height in N/m^3 superficial gas velocity in m/s and bed height in m respectively. Table 1 provides the pressure drop per unit bed height in N/m^3 superficial gas velocity in m/s and bed height in m. Every term that is part of the model has a corresponding line in this analysis of variance table. It is really helpful to every single one who has category independent variables. The number of degrees of freedom in the model decreases when this component is eliminated. There are eleven total degrees of freedom, ranging from one to nine. The numerator degrees of freedom as determined by the F-test are shown here.

Since the intercept represents the constant, it has one degree of freedom, which is standard. There are two predictors in the model, as shown by the two degrees of freedom. The model's R^2 loss is 0.8761, which indicates that it accounts for 87.61% of the variation in total. The R^2 loss for the superficial gas velocity is 0.8439, meaning that 84.39% of the variance can be explained by this variable alone. The R^2 loss for bed height is 0.0322, which indicates that 3.22% of the variation is explained by this variable[35]. The intercept, which is unimportant for understanding the predictors, is the entire sum of squares for the constant. The Sum of Squares divided by the appropriate degrees of freedom yields the Mean Square. The mean square of each prediction is compared to the mean square of the error using the F-Ratio. With an F-Ratio of 219.225, the model is considered very significant overall. The F-Ratio of 422.347 for the superficial gas velocity indicates that this factor is quite important in the model. The F-Ratio for bed height is 16.103, which is statistically significant even though it is less than the gas velocity. Both the surface gas velocity and the bed height have P-Values less than 0.0002, indicating that they are both statistically significant predictors of the dependent variable. A strong correlation between the predictors and the dependent variable is shown by values close to 0[36].

Based on the research, the bulk of the variation in the model can be explained by the dominating predictor, which is superficial gas velocity. Although it accounts for a much lower fraction of the variance, bed height also has a role. With both predictors being statistically significant, the model as a whole accounts for 87.61% of the variation in the result.

Figure 3 depicts the histogram of the residual of the of pressure drop per unit bed height in N/m^3 superficial gas velocity in m/s and bed height in m after it has been calculated. The residuals' pressure decrease per unit bed height histogram has a cantered, fairly symmetric distribution around zero. Most of the residuals lie in the range of -2000 to 2000, with a few exceptions at each extreme, especially in the negative area. The uneven heights of the bars show that the distribution is not perfectly normal, but it does imply that the residuals of the model are fairly balanced. The residuals, which fall between -4000 and 4000, suggest that the model has a small propensity to underestimate specific data and some small prediction mistakes overall[37].

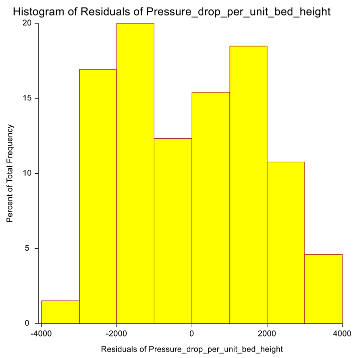

Fig. 3: Histogram of residuals of pressure drop per unit bed height in N/m^3 superficial gas velocity in m/s and bed height in m.

Table 1. Regression Coefficient T-Tests (T-Test of H0: β(i) = 0) of pressure drop per unit bed height in N/m^3 superficial gas velocity in m/s and bed height in m[33].

Independent Variable	Regression Coefficient	Standard Error Sb(i)	Standardized Coefficient	T-Statistic	P-Value	Reject H0 b(i) at α = 0.05?
Intercept	411.35	859.4857	0.0000	0.479	0.6339	No
Superficial gas velocity	147455.5	7175.069	0.9187	20.551	0.0000	Yes
Bed height	2623.57	653.7964	0.1794	4.013	0.0002	No

The residual of pressure drop per unit bed height in N/m^3, the superficial gas velocity in m/s, and the bed height in m are represented in Fig. 4 as an example of a typical probability map. The residuals of pressure drop per unit bed height often follow a linear trend, as seen by the normal probability plot, suggesting that they are roughly normally distributed. On the other hand, both tails exhibit deviations from the straight line, especially at the center fits the normal distribution well, meaning that the model residuals are normally distributed for the majority of observations[38].

Table 2. Analysis of Variance for pressure drop per unit bed height in N/m^3 superficial gas velocity in m/s and bed height in m[34].

Source	DF	R^2 Lost If Term(s) Removed	Sum of Squares	Mean Square	F-Ratio	P-Value
Intercept	1	0.8761	1.179405E^{+10}	1.179405E^{+10}	1	
Model	2		1.522749E^{+09}	7.613744E^{+08}	219.225	0.0000
Superficial gas velocity	1	0.8439	1.466824E^{+09}	1.466824E^{+09}	422.347	0.0000
Bed height	1	0.0322	5.592524E^{+07}	5.592524E^{+07}	16.103	0.0002
Error	62	0.1239	2.153278E^{+08}	3473030		
Total (Adjusted)	64		1.738077E^{+09}	2.715745E^{+07}		

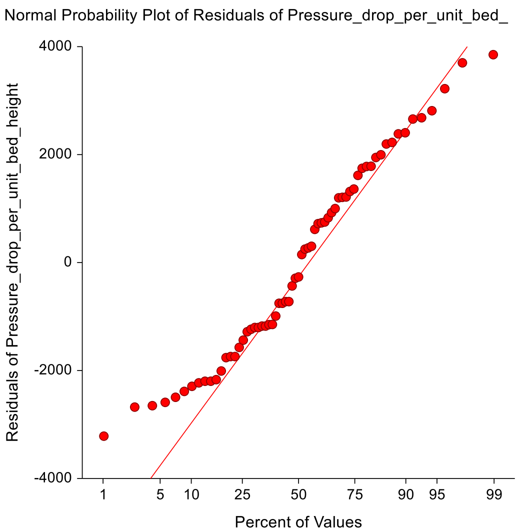

Fig. 4: Normal probability plot of residual pressure drop per unit bed height in N/m^3 superficial gas velocity in m/s and bed height in m.

3.2 Friction factor

Figure 5 depicts a three-dimensional surface plot illustrating the relationship between friction factor (f), superficial gas velocity, and bed height. A sequence of peaks and troughs on the surface show how the friction factor varies with changes in the two independent variables.

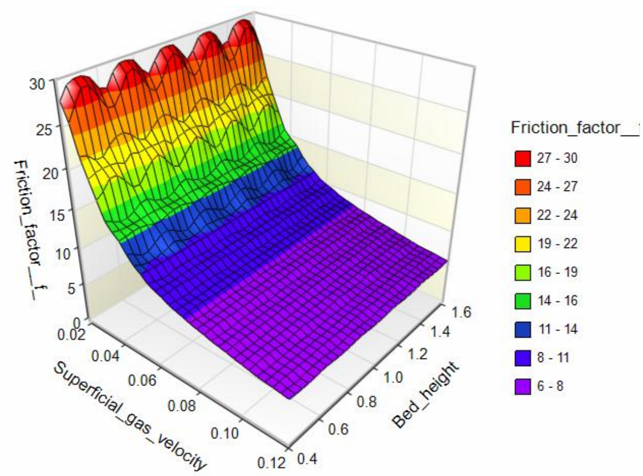

Fig. 5: Surface plot of friction factor against superficial gas velocity in m/s and bed height in m.

The friction factor tends to decrease with increasing surface gas velocity, especially at greater bed heights. On the other hand, at lower velocities, the friction factor is constant for varying bed heights. These changes are visually represented by the color gradient, which goes from red (greater friction factors) to purple (lower values).

According to this analysis, the friction factor in the system can be greatly influenced by optimizing bed height and gas velocity. For fluidized bed operations, for example, lower friction factors are preferred for efficiency. All things considered, the graph does a good job of explaining the intricate relationship between these variables and how it affects frictional resistance[39].

The friction factor (f) as a function of bed height and superficial gas velocity is shown in the graph. larger superficial gas velocities and bed heights typically result in larger friction factors, as seen by the color-coded surface plot, where purple represents the lowest values and red the highest. Understanding how variations in these factors impact the friction factor is made easier with the aid of this representation, which is essential for maximizing fluid dynamics in systems such as fluidized beds.

In fluidized beds, bed height greatly affects the friction factor. The contact area between the gas and the particles rises with bed height. The friction factor rises as a result of more interactions and collisions between the gas and the particles caused by this increased contact area. The gas must pass through more material at a higher bed height, which raises the flow resistance. Because of the greater resistance, there is a greater pressure drop over the bed, which raises the friction factor. Particle distribution may be more uniform on a taller bed, which could have an impact on the dynamics of the flow[27]. A taller bed generally tends to have a higher average friction factor, while differences in the distribution may cause the local friction factor to vary. The flow regime can transition from a fixed bed to a fluidized bed and ultimately to a turbulent or fast fluidization regime with an increase in bed height. The friction characteristics of each of these regimes vary, and as bed height increases, the friction factor typically rises as well. Comprehending these impacts is imperative in order to maximize fluidized bed performance and design, guarantee effective gas-solid interactions, and reduce energy usage[23].

Below is the approximated Equation (8) that fits the curves: f is friction factor, L is bed length, and G is super gas velocity.

$$f= 23.87 - 175.89\ G - 0.00032\ L \qquad (8)$$

The Equation 8 is generated from the experimental data for which the Fig. 5 is plotted. This shows the validation of the equation.

Table 3. Regression Coefficient T-Tests (T-Test of H0: β(i) = 0) of friction factor superficial gas velocity in m/s and bed height in m[33].

Independent Variable	Regression Coefficient	Standard Error Sb(i)	Standardized Coefficient	T-Statistic	P-Value	Reject H0 b(i) at α = 0.05?
Intercept	23.87	1.668735	0.0000	14.302	0.0000	Yes
Superficial gas velocity	-175.89	13.93076	-0.8485	-12.626	0.0000	Yes
Bed height	-0.00032	1.269379	0.0000	0.000	0.9998	No

Table 3 summarizes the results of a regression analysis, showcasing the relationship between the independent variables—superficial gas velocity and bed height—and the dependent variable. With a statistically significant t-statistic of 14.302 and a p-value of 0.0000, the intercept's coefficient of 23.87 indicates strong evidence against the null hypothesis (H0) that the intercept is zero.

With a coefficient of -175.89, superficial gas velocity, one of the independent variables, significantly affects the dependent variable negatively. Its associated p-value of 0.0000 and t-statistic of -12.626 provide strong evidence to reject the null hypothesis, indicating that a significant reduction in the dependent variable is caused by increased surface gas velocity[40].

In contrast, a t-statistic close to zero and a p-value of 0.9998 accompany bed height's coefficient of -0.00032, suggesting that it has no discernible effect on the dependent variable. Consequently, we are unable to reject the bed height null hypothesis, indicating that it makes no significant contribution to the model. Overall, the findings highlight how crucial surface gas velocity is in determining the result, with bed height appearing to be insignificant[28].

Table 4 shows the findings of the regression model's analysis of variance (ANOVA), which evaluated the impact of bed height and surface gas velocity on the dependent variable. A strong match is shown by the R^2 value, which shows that the model accounts for roughly 72% of the variability in the data. The model's mean square is 1043.529 and its total of squares is 2087.058, resulting in an F-ratio of 79.707. Given the high F-ratio and matching p-value of 0.0000, it can be concluded that the model as a whole is statistically significant[28].

With an F-ratio of 159.415 and a p-value of 0.0000, surface gas velocity exhibits a significant contribution to the model when individual terms are examined, supporting the importance of this term in predicting the dependent variable and justifying rejection of the null hypothesis. Bed height, on the other hand, has a negligible contribution to the model; its p-value of 0.9988 and F-ratio are both close to zero.

The remaining variability is explained by the error term, which has 62 degrees of freedom and a sum of squares of 811.7039. Overall, these findings point to the importance of superficial gas velocity and indicate that bed height has little effect on the regression analysis's conclusion.

Using yellow bars to represent frequency, the histogram (Fig. 6) shows the distribution of residuals for the friction factor (f). The residual values, which span from -5 to 11, are represented by the x-axis, and the number of observations falling within each residual range is indicated by the y-axis[38].

Table 4. Analysis of Variance for friction factor superficial gas velocity in m/s and bed height in m[34].

Source	DF	R^2 Lost If Term(s) Removed	Sum of Squares	Mean Square	F-Ratio	P-Value
Intercept	1		8475.804	8475.804		
Model	2	0.7200	2087.058	1043.529	79.707	0.0000
Superficial gas velocity	1	0.7200	2087.058	2087.058	159.415	0.0000
Bed height	1	0.0000	8.482957E-07	8.482957E-07	0.000	0.9998
Error	62	0.2800	811.7039	13.092		
Total (Adjusted)	64		2898.762	45.29315		

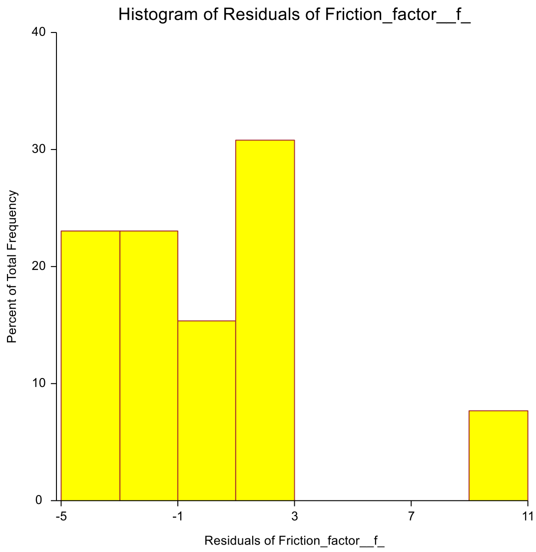

Fig. 6: Histogram of residuals of friction factor, superficial gas velocity in m/s and bed height in m.

With bars centered between -5 and -1, the histogram has a skewed distribution, indicating that the majority of residuals cluster in this region. Higher residual values show a discernible decline in frequency, which suggests fewer observations. The fact that the data doesn't seem to follow a normal distribution could mean that the model isn't capturing all of the underlying relationships or trends in the dataset.

Overall, the inclusion of both positive and negative residuals indicates heterogeneity in the model's performance across different observations, even if the bulk of residuals are negative, indicating that the observed values are smaller than the anticipated values. This distribution calls for additional research to evaluate the suitability of the model and pinpoint areas for improvement.

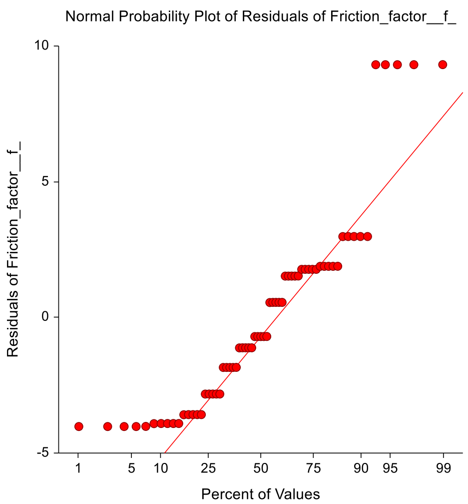

Fig. 7: Normal probability plot of residual friction factor, superficial gas velocity in m/s and bed height in m.

The distribution of the friction factor residuals against the predicted values under a normal distribution is shown on the graph, which is a Normal Probability Plot of the residuals (Fig. 7). As the residuals get closer to the extremes, the points mostly exhibit a curved shape, which is especially apparent in the lower percentiles and indicates deviations from normalcy. The residuals appear to be non-normally distributed, despite the fact that certain spots in the center are almost exactly aligned with the diagonal reference line. This could indicate problems with the model's fit or underlying assumptions. This analysis emphasizes the necessity of looking at the residuals more thoroughly and perhaps reevaluating the friction factor model[24].

3.3 Power consumed by the bed

The link between bed height, superficial gas velocity, and power consumption in a fluidized bed system is depicted in Fig. 8. Warmer colors denote larger power requirements, while the color gradient shows different power levels. The surface exhibits a general increasing trend as bed height rises, indicating that higher bed heights are associated with higher power usage. The graphic also shows how variations in surface gas velocity affect power requirements, suggesting a complicated relationship between these factors. This graphic emphasizes how crucial it is to maximize gas velocity and bed height in order to improve system efficiency[32].

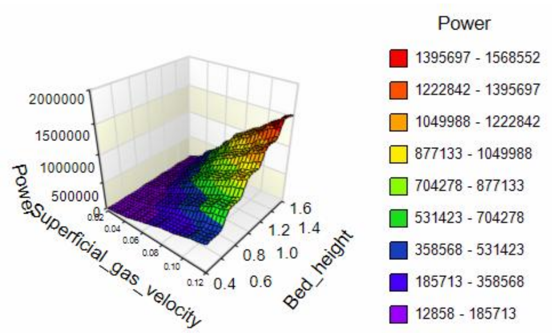

Fig. 8: Surface plot of power consumed against superficial gas velocity in m/s and bed height in m.

The contour plot shows the contours of power consumption across various combinations of these parameters by displaying the link between bed height and superficial gas velocity. The color gradient denotes different power levels; brighter colors indicate higher power consumption, and darker colors indicate lower power requirements. Power consumption increases with bed height, especially at greater surface gas velocities which is supported by the surface plot of Fig. 8. The contours show the necessity for careful optimization in fluidized bed operations to achieve desired performance while limiting energy use, as some combinations of bed height and gas velocity might result in noticeably greater power needs.

Below is the approximated Equation (9) that fits the curves: Q is power, L is bed length, and G is super gas velocity.

$$Q = -8x10^5 + 1.04x10^7 G + 574106.6 L \quad (9)$$

The Equation 9 is generated from the experimental data for which the Fig. 8 is plotted. This shows the validation of the equation.

Table 5. Regression Coefficient T-Tests (T-Test of H0: β(i) = 0) of power consumed superficial gas velocity in m/s and bed height in m[33].

Independent Variable	Regression Coefficient	Standard Error Sb(i)	Standardized Coefficient	T-Statistic	P-Value	Reject H0 b(i) at α = 0.05?
Intercept	-799885.9	61888.43	0.0000	-12.925	0.0000	Yes
Superficial gas velocity	1.04*E+07	13.93076	-0.8485	-12.626	0.0000	Yes
Bed height	574106.6	1.269379	0.0000	0.000	0.9998	Yes

The T-Test findings for the null hypothesis across three independent variables in a regression analysis are shown in the Table 5. The coefficients' T-Statistics and P-Values demonstrate that each predictor—Intercept, Superficial Gas Velocity, and Bed Height—is statistically significant. Notably, the null hypothesis is rejected due to the Intercept's coefficient of -799885.9, T-Statistic of -12.925, and P-Value of 0.0000. Similar to this, Bed Height likewise demonstrates relevance with a coefficient of 574106.6, T-Statistic of 12.195, and P-Value of 0.0000, while Superficial Gas Velocity shows a strong positive link with a coefficient of 1.04E+07, T-Statistic of 20.090, and P-Value of 0.0000. At the 0.05 significance level, these data collectively imply that all three variables have a substantial impact on the dependent variable.

Table 6 provides an overview of the several sources that contribute to a model's analysis of variance and shows how the R^2 statistic, which measures the overall model fit, is affected when certain elements are removed. A large amount of variability may be explained by the intercept alone, which has a lost sum of squares of 1.682535E+13. With an F-Ratio of 276.164 and a P-Value of 0.0000, the combined model that accounts for both Superficial Gas Velocity and Bed Height is statistically significant in explaining the variance in the dependent variable [24].

The bulk of the residuals fall between -200,000 and 200,000, exhibiting a broadly symmetrical distribution centered around zero in the power residuals histogram (Fig. 9). While there is a sizable spread on either side that suggests some fluctuation, the height of the bars indicates a considerable concentration of values in the midway, indicating that most power projections are reasonably accurate. A well-fitting model is suggested by the absence of severe outliers, which shows that the residuals stay within a tolerable range. The distribution is generally well-illustrated by the yellow bars, which also emphasize the equilibrium between positive and negative residuals.

Table 6. Analysis of Variance for power consumed superficial gas velocity in m/s and bed height in m[34].

Source	DF	R^2 Lost If Term(s) Removed	Sum of Squares	Mean Square	F-Ratio	P-Value
Intercept	1		1.682535E+13	1.682535E+13		
Model	2	0.8991	9.945981E+12	4.972991E+12	276.164	0.0000
Superficial gas velocity	1	0.6570	7.267994E+12	7.267994E+12	403.612	0.0000
Bed height	1	0.2421	2.677987E+12	2.677987E+12	148.716	0.0000
Error	62	0.1009	1.116456E+12	1.800736E+10		
Total (Adjusted)	64		1.106244E+13	1.728506E+11		

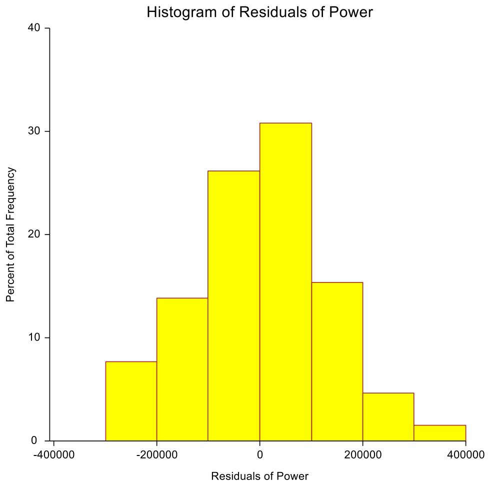

Fig. 9: Histogram of residuals of power consumed superficial gas velocity in m/s and bed height in m.

The residuals of power show a nearly linear connection along the reference line in the normal probability plot, suggesting that the residuals are roughly normally distributed (Fig. 10). The majority of the data points, especially in the middle regions, cluster tightly around the line, indicating a very symmetric distribution of the model's errors. On the other hand, a small departure from linearity at both the higher and lower ends of the plot suggests that there may be some moderate outliers and possible skewness. This graphic aligns with the assumption of residual normality, essential for validating the statistical model underpinning the investigation.

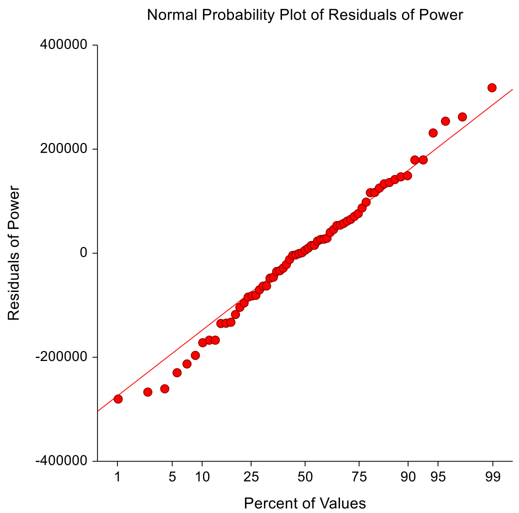

Fig. 10: Normal probability plot of residual power consumed superficial gas velocity in m/s and bed height in m.

3.4 Coefficient of drag

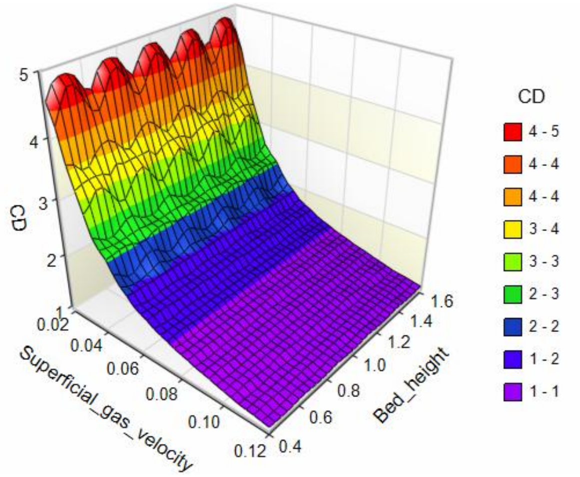

Fig. 11: surface plot of drag coefficient against superficial gas velocity in m/s and bed height in m.

The link between bed height, superficial gas velocity, and the accompanying CD which can be a dimensionless quantity or coefficient associated with flow or reaction is depicted in the three-dimensional surface plot (Fig. 11). The peak regions which are highlighted in red and orange indicate that greater CD values occur at moderate gas velocity and bed height levels, indicating ideal circumstances for boosting flow rates or reaction efficiencies. When gas velocity drops or bed height rises above a particular threshold, the CD values dramatically decline and change to colder hues like purple and blue, which denote less efficient performance. This pattern draws attention to how the two variables interact and underscores the necessity of cautious optimization in applications where there are interactions between gas and solid.

The link between bed height and surface gas velocity in relation to the coefficient of drag (CD) is represented by contour lines on the graph. The contours change towards lower CD values, indicating a noticeable decrease in CD as surface gas velocity increases, particularly at lower bed heights. This pattern is emphasized by the color gradient, where warmer hues—like yellow and red—indicate greater CD values and cooler hues—like blue and green—indicate lower values. This indicates that elevated gas velocities and reduced bed heights are optimal for minimizing drag, potentially impacting fluidization processes in chemical and environmental engineering contexts.

Below is the approximated Equation (10) that fits the curves: Coefficient of drag C, L is bed length, and G is super gas velocity.

$$C= 3.95 - 28.17\ G + 0.0006\ L \qquad (10)$$

The Equation 10 is generated from the experimental data for which the Fig. 11 is plotted. This shows the validation of the equation.

Table 7. Regression Coefficient T-Tests (T-Test of H0: β(i) = 0) of coefficient of drag (CD) superficial gas velocity in m/s and bed height in m.

Independent Variable	Regression Coefficient	Standard Error Sb(i)	Standardized Coefficient	T-Statistic	P-Value	Reject H0 b(i) at α = 0.05?
Intercept	3.95	0.267133	0.0000	14.756	0.0000	Yes
Superficial gas velocity	-28.17	2.230052	-0.8486	-12.632	0.0000	Yes
Bed height	-0.0006	0.2032036	-0.0002	-0.003	0.9976	No

The T-test findings, which evaluated the null hypothesis that every regression coefficient is equal to zero, are summarized in the Table 7. With a T-statistic of 14.756 and a P-value of 0.0000, the intercept has a significant positive coefficient of 3.95, providing compelling evidence to reject the null hypothesis at the 0.05 significance level. Conversely, the variable superficial gas velocity exhibits a coefficient of -28.17, a T-statistic of -12.632, and a P-value of 0.0000, all of which lead to the rejection of the null hypothesis and indicate a significant influence of this variable on the dependent variable. As an indication that bed height does not substantially affect the response variable in this model, bed height has a coefficient of -0.0006 with a T-statistic of -0.003 and a P-value of 0.9976, indicating that there is insufficient data to reject the null hypothesis at the same significance level.

Table 8. Analysis of Variance for coefficient of drag (CD) superficial gas velocity in m/s and bed height in m.

Source	DF	R^2 Lost If Term(s) Removed	Sum of Squares	Mean Square	F-Ratio	P-Value
Intercept	1		246.5389	246.5389		
Model	2	0.7202	53.53377	26.76689	79.783	0.0000
Superficial gas velocity	1	0.7202	53.53377	53.53377	159.566	0.0000
Bed height	1	0.0000	3.076923E-06	3.076923E-06	0.000	0.9976
Error	62	0.2798	20.8007	0.3354951		
Total (Adjusted)	64		74.33447	1.161476		

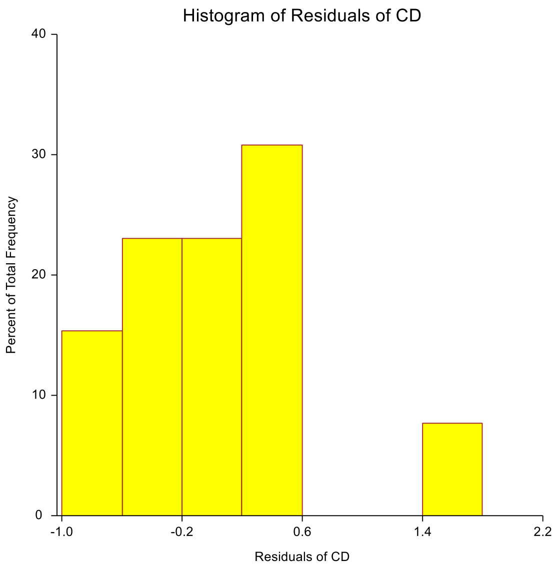

Fig. 12: Histogram of residuals of coefficient of drag (CD), superficial gas velocity in m/s and bed height in m.

The regression model's analysis of variance (ANOVA), which focuses on the various terms' contributions to the overall model fit, is shown in the Table 8. With an F-Ratio of 79.783 and a P-value of 0.0000, the model explains a large amount of the variation, suggesting that at least one predictor significantly enhances the model. In particular, the elimination of superficial gas velocity highlights its crucial function in the model by causing a significant loss in R^2 (0.7202) and a high F-Ratio of 159.566 with a P-value of 0.0000. On the other hand, a P-value of 0.9976 indicates that bed height has little effect, indicating that eliminating it has no discernible impact on the explained variation. All things considered, the model seems strong, mostly due to the contributions of the superficial gas velocity instead of the bed height.

Key information about the performance of the model can be found in the residuals histogram for the coefficient of drag (Fig. 12). With most residuals ranging between -1.0 and 1.0, the distribution looks roughly normal, suggesting that the model fits the data well and doesn't have any notable biases. A significant percentage of the projected values appear to match the actual data quite closely, as seen by the peak at 0.6. On the other hand, the small bias towards negative residuals may indicate some underestimating in some cases. The histogram as a whole show that although the model does a good job of capturing the trend, it might be improved to better account for data variations or outliers.

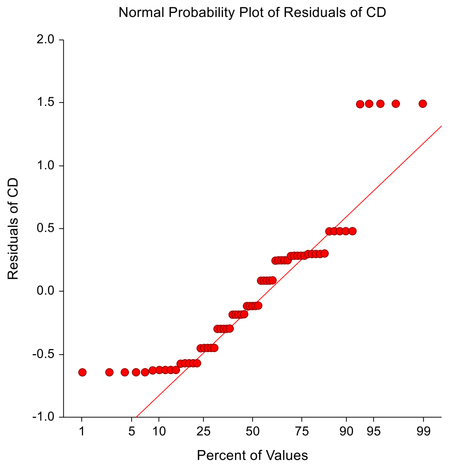

Fig. 13: Normal probability plot of residual coefficient of drag (CD) superficial gas velocity in m/s and bed height in m.

The distribution of residuals with respect to a theoretical normal distribution is shown by the normal probability plot of the coefficient of drag residuals (Fig. 13). When the % of values increases, the data points depart from the diagonal line, especially in the upper range, but at the lower percentiles, they closely follow it, suggesting that many residuals are normally distributed. This shows that even while the model works well for the majority of predictions, there may be problems capturing high values, which could cause the residual distribution to become somewhat non-normal. These variances might point to the existence of outliers or the necessity for additional research into the model's underlying presumptions in order to enhance fit and accuracy.

4. Conclusion

The research on fluidized bed systems offers significant insights into the intricate interactions between gas and solid particles, highlighting the essential influence of bed height and superficial gas velocity on system performance. The principal results derived from the research encompass. The investigation indicates that surface gas velocity significantly influences pressure drop and friction factor in the fluidized bed. Elevated gas velocities enhance interactions between gas and particles, culminating in augmented flow resistance and pressure drop across the bed. The height of the bed influences the friction factor and flow dynamics, but its impact on the overall model is less substantial than that of gas velocity. The results demonstrate that alterations in bed height exert a negligible influence on pressure drop, indicating that adjusting gas velocity is paramount for improving fluidized bed efficacy. The research highlights the importance of a meticulously built experimental framework for precisely examining fluid dynamics in particle beds. The implementation of transparent columns and accurate measurement instruments facilitates the effective observation of flow properties, crucial for confirming theoretical models and enhancing practical applications. The findings from this research are relevant to multiple industrial processes, such as catalytic reactions, coal combustion, and material drying. Comprehending the hydrodynamics of fluidized beds can result in optimized reactor designs, increased efficiency, and diminished energy consumption in various applications. This work enhances the existing information on fluidized bed technology, establishing a basis for future research and development focused on optimizing these systems for industrial applications. Additional research on the impact of particle size distribution and other operational parameters may improve the comprehension and efficacy of fluidized beds across many applications.

Future research may concentrate on many specific avenues in this area. A promising field of research is the examination of non-spherical particles, which may elucidate the influence of particle morphology on behavior and interactions within diverse systems. Broadening the spectrum of velocities examined may provide significant insights, particularly in scenarios where extreme velocities are pivotal to system efficacy. Furthermore, investigating alternative regression models, including machine learning methodologies, may enhance the precision and relevance of predictive studies. This amalgamation of developments would improve the comprehension and simulation of intricate physical and chemical events.

References

1) Chen, S., Verding, J., Lang, X., Ouyang, Y., Heynderickx, G. J., & Van Geem, K. M. Chen, Siyuan, et al. "Advances in design of internals: Applications in conventional and process intensification units." Chemical Engineering and Processing-Process Intensification 201 109806 (2024). doi:10.1016/j.cep.2024.109806.
2) Rhodes, Martin J., and Jonathan Seville. Introduction to particle technology. John Wiley & Sons, (2024). https://books.google.com.om/books/about/Introduction_to_Particle_Technology.html?id=D70IEQAAQBAJ&redir_esc=y (Accessed October 5, 2024).
3) Reed III, T. M., and M. R. Fenske. "Effects of agitation on gas fluidization of solids." Industrial & Engineering Chemistry 47(2) 275-282 (1955). doi:10.1021/ie50542a032.
4) Neogi, Ajita, Hare K. Mohanta, and Priya C. Sande. "Study of fluidized bed freeboard for effect of Geldart A particles shape using particle image velocimetry (PIV)." Powder Technology 433 119235 (2024). doi:10.1016/j.powtec.2023.119235.
5) Zapater, D., et al. "Multifunctional fluidized bed reactors for process intensification." Progress in Energy and Combustion Science 105 101176 (2024). doi:10.1016/j.pecs.2024.101176.
6) Devan, Chaithanya P., et al. "Investigating the influence of design parameters on the flow characteristics of a rectangular gas-solid fluidized bed

with non-spherical particles." Multiscale and Multidisciplinary Modeling, Experiments and Design 1-19 (2024). doi:10.1007/s41939-024-00499-z
7) van der Sande, P. C., et al. "Fluidization behavior of stirred gas–solid fluidized beds: A combined X-ray and CFD–DEM–IBM study." Chemical Engineering Journal 499 155944 (2024). doi:10.1016/j.cej.2024.155944.
8) Razzak, Shaikh A. "Characteristics and diverse applications of (gas)-liquid-solid circulating fluidized beds: A comprehensive review." Powder Technology 119359 (2024). doi:10.1016/j.powtec.2024.119359.
9) Varghese, Mona Mary, et al. "Experimental investigation of the behavior of non-spherical particles in a small-scale gas-solid fluidized bed." Flow Measurement and Instrumentation 95 102493 (2024). doi:10.1016/j.flowmeasinst.2023.102493.
10) Wieczorek, Martyna N., Wei Zhou, and Janusz Pawliszyn. "Perspective on sample preparation fundamentals." Advances in Sample Preparation 10 100114 (2024). doi:10.1016/j.sampre.2024.100114.
11) Askaripour, Hossein, and Asghar Molaei Dehkordi. "Effects of initial static bed height on fractional conversion and bed pressure drop in tapered-in and tapered-out fluidized bed reactors." International Journal of Multiphase Flow 79 50-61 (2016). doi:10.1016/j.ijmultiphaseflow.2015.08.006.
12) Kaewklum, Rachadaporn, Vladimir I. Kuprianov, and Peter L. Douglas. "Hydrodynamics of air–sand flow in a conical swirling fluidized bed: A comparative study between tangential and axial air entries." Energy Conversion and Management 50(12) 2999-3006 (2009). doi:10.1016/j.enconman.2009.07.019.
13) Ju, Youngsan, and Chang-Ha Lee. "Dynamic modeling of a dual fluidized-bed system with the circulation of dry sorbent for CO2 capture." Applied Energy 241 640-651 (2019). doi:10.1016/j.apenergy.2019.03.070.
14) Wei, Bangji, et al. "Effects of tube configurations on the heat transfer and hydrodynamic behavior in a gas-solid fluidized bed." Powder Technology 436 119439 (2024). doi:10.1016/j.powtec.2024.119439.
15) Wu, Gongpeng, Hongkai Tong, and Yan He. "Characteristics of local flow structure with different particle properties in a gas-solid diameter-varying fluidized bed." Powder Technology 433 119202 (2024). doi:10.1016/j.powtec.2023.119202.
16) Cai, Min, et al. "Hydrodynamics and OCM reaction performance in a bubbling fluidized bed reactor and a riser reactor." Particuology 86 188-204 (2024). doi:10.1016/j.partic.2023.05.008.
17) Escudero, David, and Theodore J. Heindel. "Bed height and material density effects on fluidized bed hydrodynamics." Chemical Engineering Science 66(16) 3648-3655 (2011). doi:10.1016/j.ces.2011.04.036.
18) Khan, A. R., and J. F. Richardson. "The resistance to motion of a solid sphere in a fluid." Chemical Engineering Communications 62(1-6) 135-150 (1987). doi:10.1080/00986448708912056
19) He, Jiawei, Ruiqi Lei, and Le Xie. "Customized Software Package for the Simultaneous Prediction of Multiple Fluidization Characteristic Parameters in Liquid–Solid Fluidized Beds." Industrial & Engineering Chemistry Research 63(28) 12656-12669 (2024). doi:10.1021/acs.iecr.4c01006.
20) Huang, Yaqin, et al. "Numerical prediction on minimum fluidization velocity of a supercritical water fluidized bed reactor: Effect of particle shape." Powder Technology 403 117397 (2022). doi:10.1016/j.powtec.2022.117397.
21) Ansari, Amir, et al. "Modeling average pressure and volume fraction of a fluidized bed using data-driven smart proxy." Fluids 4(3) 123 (2019). doi:10.3390/fluids4030123.
22) Saleh, Esam Ahmed, et al. "Development of Novel Dimensionless Parameters for Accurate Estimation of Properties in Fluidized Beds." Iran. J. Chem. Chem. Eng. (IJCCE) Research Article Vol 43(5) (2024). doi:10.30492/ijcce.2023.2010041.6188.
23) Chiarla, S. “CFD simulation of gas-solid hydrodynamics in a high-pressure fluidized bed (Doctoral dissertation”, Politecnico di Torino), (2024).
24) Li, Shuyue, et al. "Multi-scale simulation of particle density effects on hydrodynamics in dense gas-solid fluidized beds." Powder Technology 435 119394 (2024). doi:10.1016/j.powtec.2024.119394.
25) Kamble, L. V., D. R. Pangavhane, and T. P. Singh. "Experimental investigation of horizontal tube immersed in gas–solid fluidized bed of large particles using artificial neural network." International Journal of Heat and Mass Transfer 70 719-724 (2014). doi.org/10.1016/j.ijheatmasstransfer.2013.11.073.
26) Li, Guang, et al. "Application of general regression neural network to model a novel integrated fluidized bed gasifier." International Journal of Hydrogen Energy 43(11) 5512-5521 (2018). doi:10.1016/j.ijhydene.2018.01.130.
27) Ma, Z., R. D. Whitley, and N-HL Wang. "Pore and surface diffusion in multicomponent adsorption and liquid chromatography systems." AIChE Journal 42(5) 1244-1262 (1996). doi:10.1002/aic.690420507.
28) Weber, Thomas W., and Ranjit K. Chakravorti. "Pore and solid diffusion models for fixed-bed adsorbers." AIChE Journal 20(2) 228-238 (1974). doi:10.1002/aic.690200204.
29) Furuya, Eiji, Yasushi Takeuchi, and Kenneth E. Noll. "Intraparticle diffusion of phenols within bidispersed macroreticular resin particles." Journal of chemical engineering of Japan 22(6) 670-676 (1989). doi:10.1252/jcej.22.670.

30) Bautista, L. F., M. Martinez, and J. Aracil. "Adsorption of α-amylase in a fixed bed: Operating efficiency and kinetic modeling." AIChE Journal 49(10) 2631-2641 (2003). doi:10.1002/aic.690491016.
31) Ghorai, Subhashini, and K. K. Pant. "Investigations on the column performance of fluoride adsorption by activated alumina in a fixed-bed." Chemical Engineering Journal 98 (1-2) 165-173 (2004). doi:10.1016/j.cej.2003.07.003.
32) Sotelo, J. L., et al. "Adsorption of methyl ethyl ketone and trichloroethene from aqueous solutions onto activated carbon fixed-bed adsorbers." Separation and Purification Technology 37(2) 149-160 (2004). doi:10.1016/j.seppur.2003.09.006.
33) Babu, B. V., and A. S. Chaurasia. "Modeling, simulation and estimation of optimum parameters in pyrolysis of biomass." Energy Conversion and Management 44(13) 2135-2158 (2003). doi:10.1016/S0196-8904(02)00237-6.
34) Babu, B. V., and A. S. Chaurasia. "Modeling for pyrolysis of solid particle: kinetics and heat transfer effects." Energy Conversion and Management 44(14) 2251-2275 (2003). doi:10.1016/S0196-8904(02)00252-2.
35) Babu, B. V., and A. S. Chaurasia. "Parametric study of thermal and thermodynamic properties on pyrolysis of biomass in thermally thick regime." Energy Conversion and Management 45(1) 53-72 (2004). doi:10.1016/S0196-8904(03)00130-4.
36) Babu, B. V., and A. S. Chaurasia. "Dominant design variables in pyrolysis of biomass particles of different geometries in thermally thick regime." Chemical Engineering Science 59(3) 611-622 (2004). doi:10.1016/j.ces.2003.10.014.
37) Babu, B. V., and A. S. Chaurasia. "Pyrolysis of biomass: improved models for simultaneous kinetics and transport of heat, mass and momentum." Energy conversion and Management 45(9-10) 1297-1327 (2004). doi:10.1016/j.enconman.2003.09.013.
38) Babu, B. V., and A. S. Chaurasia. "Heat transfer and kinetics in the pyrolysis of shrinking biomass particle." Chemical Engineering Science 59(10) 1999-2012 (2004). doi:10.1016/j.ces.2004.01.050.
39) Rasteh, Mojtaba, Fatola Farhadi, and Alireza Bahramian. "Hydrodynamic characteristics of gas–solid tapered fluidized beds: Experimental studies and empirical models." Powder Technology 283 355-367 (2015). doi:10.1016/j.powtec.2015.06.002.
40) Saleh, Esam Ahmed, et al. "Development of Novel Dimensionless Parameters for Accurate Estimation of Properties in Fluidized Beds." Iran. J. Chem. Chem. Eng. (IJCCE) Research Article Vol 43(5) (2024). doi:10.30492/ijcce.2023.2010041.6188.